Nuclear Materials and Energy 45 (2025) 102022

Contents lists available at ScienceDirect

Nuclear Materials and Energy

journal homepage: www.elsevier.com/locate/nme

Water-cooled lead and ceramic breeder (WLCB) breeding blanket (BB) for the EU DEMO: Neutronic campaigns for T breeding optimization☆

Iole Palermo [a,*], Francisco A. Hernandez [b], Salvatore D'Amico [c], Jin Hun Park [b], Pavel Pereslavtsev [b], Guangming Zhou [b], Iñaki Zumalde [a,d]

[a] CIEMAT, Fusion Technology Division, Avda. Complutense 40, 28040 Madrid, Spain
[b] Karlsruhe Institute of Technology (KIT), 76131 Eggenstein-Leopoldshafen, Germany
[c] Consortium EUROfusion, Boltzmannstr. 2, Garching 85748, Germany
[d] Universidad Autónoma de Madrid, Facultad de Ciencias, 28049 Madrid, Spain

ARTICLE INFO

Keywords:
Ceramic breeder materials
Tritium Breeding
Neutron multiplier materials
WLCB BB
Nuclear fusion

ABSTRACT

A novel Breeding Blanket (BB) concept, the Water-cooled Lead and Ceramic Breeder (WLCB) BB, has been developed under the EUROfusion Programme to address key challenges identified during the Pre-Conceptwual Design (PCD) phase for the driver BB concepts: Water-Cooled Lithium Lead (WCLL) and Helium-Cooled Pebble Bed (HCPB). The WLCB design represents an alternative hybrid approach, combining advantageous features of both WCLL and HCPB to mitigate their respective limitations: (1) shielding inefficiencies, challenging neutron multiplier technology, and integration concerns in HCPB; (2) challenges with tritium extraction from PbLi in WCLL variants; and (3) the reliance on anti-permeation barriers. In lieu of beryllium, alternative neutron multipliers—particularly lead—have been explored.

This work focuses on the neutronic optimization of the WLCB concept, with an emphasis on tritium breeding performance. Extensive neutronic simulation campaigns were conducted to optimize key design parameters, including toroidal and radial blanket layouts, cooling plate dimensions and water content, neutron multiplier zoning and materials (Pb, $Be_{12}Ti$, Zr_5Pb_3, C, ZrH_2), ^6Li enrichment, ceramic breeder material, ceramic packing factor, and First Wall (FW) design to achieve the best results in terms of Tritium Breeding Ratio (TBR).

The resulting preliminary design – based on the best balance between neutronic performances and viability considerations, among others – achieves the EU DEMO TBR target of 1.15, representing a promising candidate for further development and integration into future design iterations.

1. Introduction

The breeding blanket (BB) is a crucial component of any D-T fusion power plant, ensuring tritium self-sufficiency, electricity generation via heat extraction, and shielding of in-vessel components.

Designing breeding blankets is particularly challenging due to the extremely demanding conditions they must endure during operation. These include exposure to extreme temperatures and intense radiation, which leads to heat loads, material damage, transmutation, and activation. Additionally, the BB faces mechanical deformation, stress, corrosion, erosion, and cyclic loading. It must also contend with issues of chemical compatibility, isotope permeation through structural and functional materials, and the influence of strong magnetic fields. All these factors significantly complicate material selection, structural integrity, thermal management, and long-term performance, making BB design a highly complex multidisciplinary task.

Among several BB concepts, the solid breeder blanket is one of the most investigated concept for many international programmes as ITER TBM and DEMO. This concept allows to reach very high tritium production specially thanks to the Be neutron multiplier and high safety standards with a chemical inert gas (like helium) as coolant.

Europe has developed the Helium Cooled Pebble Bed (HCPB) BB being one of the two concepts selected as a "*driver blanket*" together with the Water-Cooled Lithium Lead (WCLL) BB for the European DEMOnstration reactor (EU DEMO) in 2017 to align the TBM and DEMO BB programmes [1,2].

☆ This article is part of a special issue entitled: 'PRD activities' published in Nuclear Materials and Energy.

* Corresponding author.
E-mail address: iole.palermo@ciemat.es (I. Palermo).

https://doi.org/10.1016/j.nme.2025.102022
Received 4 July 2025; Received in revised form 31 October 2025; Accepted 4 November 2025
Available online 5 November 2025

Despite progress in design and performances, challenges persist for both concepts. In the HCPB case, these stem primarily from beryllium's toxicity, high cost, scarcity, and the limited operational experience with helium cooling systems. For the WCLL concept, the issues are the complexity of circulating the entire PbLi inventory throughout the tokamak building, uncertainties in tritium extraction processes, and integration challenges related to the Tritium Extraction and Recovery (TER) system from PbLi. Additional concerns include full reliance on tritium anti-permeation coatings, critical in water-cooled systems, the low reliability of the WCLL architecture, and the potential risks associated with water–PbLi chemical reactions during accident scenarios.

To address all these questions, alternative concepts have emerged as part of the activities performed inside the Working Package Breeding Blanket (WPBB) among the recent constituted FP9 Eurofusion Programme – Horizon Europe, studying alternative BB configurations, aimed at overcoming the open issues that emerged at the end of the Pre-Conceptual Design (PCD) phase.

For that, a new concept, the so-called Water-cooled Lead and Ceramic Breeder (WLCB) Breeding Blanket, which is a hybrid between the WCLL and HCPB concepts, has been developed [3]. The idea was conceived as a best trade-off between HCPB and WCLL to avoid or mitigate:

- current issues in HCPB with low shielding, use of Be multiplier technology, and integration challenges of He piping
- current issues with T-extraction technology from PbLi in WCLL variants
- full reliance on the use of anti-permeation barriers with very high permeation reduction factor in WCLL
- uncertainties in the water-PbLi interaction during accidents.

By exploring alternative n-multipliers as lead (Pb) or Pb-alloys instead of beryllium/beryllides would allow this concept to be adapted for use with water as a coolant, avoiding the potential safety issue associated with an exothermic hydrogen-producing reaction between beryllium and water in the event of water leakage into the breeding zone (BZ). Furthermore, water is compatible with the ceramic breeder, avoiding the exothermic hydrogen-producing reaction between water and lithium–lead that could occur during a water leak in a WCLL blanket that uses lithium–lead as the breeder.

In the frame of FP9, two variants of the WLCB have been preliminary conceived: one adopting a poloidal distribution of cooling plates and ceramic breeder tubes [4,5], soon discarded due to the poor Tritium breeding performances, and another – in which it has been centered the present work- as vertical cassettes alternating the Advanced Ceramic Breeder (ACB) and the neutron multiplier (Pb, in first instance) separated by vertical cooling plates (steel cooled by water).

The purpose of this study has been to perform a comprehensive neutronic campaign in order to find a proper configuration that maximize the Tritium Breeding Ratio (TBR), the most important metric for the fuel self-sufficiency and viability of a fusion reactor. Hence, a number of parametric studies have been carried out grouped into three main campaigns for the years 2022–2025:

– Campaign 2022–23 (Section 4)

During this campaign, five main studies were carried out, focusing on optimizing the geometry and material distribution in the blanket structure:

(1) Adjustment of ACB and Pb layer geometry (investigation of the optimal thickness combination and number of layers in the repeated unit structure).
(2) Resizing of ACB layers in the rear zone (partial replacement of Pb with ACB in the back region).
(3) ACB resizing with reflector integration (rearrangement of ACB layers in the back zone with the addition of reflectors ($Be_{12}Ti$ or graphite) replacing Pb).
(4) Full reflector layer at the rear (implementation of reflectors as a continuous layer at the back, instead of being interleaved within the ACB structure).
(5) Radial resizing of the rear zone (redesign of the rear zone dimensions to assess radial optimization).

In total, 30 configurations were developed and analyzed as part of this initial campaign. The most promising configuration, referred to as *baseline2022*, was selected for further optimization in subsequent campaigns. This reference model is described in detail in Section 4, along with nuclear heating profiles that were calculated to support upcoming thermal–hydraulic analyses.

– Campaign 2023–24 (Section 5)

Building on the *baseline2022* WLCB configuration, this campaign focused on further enhancing the design by exploring a range of modifications. The following studies were conducted:

(1) Analysis of the impact of varying water content in the Cooling Plates (CP)
(2) Evaluation of different levels of ^{6}Li enrichment
(3) Testing different CP thicknesses in the front and rear blanket zones
(4) Introduction of multiplier block at the front side using two different materials, varying block sizes and CP thicknesses
(5) Partial replacement of $Be_{12}Ti$ in the rear zone (with ACB while testing different packing factors (PF))
(6) Exploration of different PF values in both front and rear zones
(7) Rear ACB replacement with Li_8PbO_6 (OctaLithium Plumbate, OLP) testing several PF.
(8) Partial replacement of $Be_{12}Ti$ in the rear zone with OLP
(9) Front ACB substitution with OLP (assessment of OLP as an alternative breeder in the front zone).

In total 63 configurations have been developed and assessed throughout this campaign.

– Campaign 2024–25 (Section 6):

As a continuation of the optimization efforts, this campaign explored both novel solutions and previously tested concepts from earlier campaigns, applied in slightly revised configurations. A total of 59 models were developed, and the following studies were conducted:

(1) Modification of the front unit layout (a parametric study was performed using a fixed 1 cm ACB layer and varying the Pb layer thickness from 1 cm to 9 cm). Based on the most promising configuration identified here additional tests were conducted, including:
(2) Extension of the new unit layout to the rear zone. This led to the definition of a new reference configuration, termed *baseline2024*.
(3) Use of ACB in the rear zone without a neutron multiplier
(4) Replacement of beryllide with alternative neutron multipliers and reflectors (specifically, Pb, C, and ZrH_2 were tested in the rear zone).
(5) Alternative breeder compositions (evaluation of 100 % OLP in the rear zone, and a 50 % ACB + 50 % OLP mixture in the front zone).
(6) Cooling Plate thickness variation (increased from 5 mm to 7–8 mm)
(7) First Wall (FW) modification (introducing an additional 1 cm ACB layer in the front).

(8) Structural enhancement (addition of a 2 cm toroidal steel stiffener to improve mechanical feasibility and evaluate neutronic impact).

Following the results of the previous campaigns, a final reference configuration was developed by combining the most promising and/or necessary design options to achieve an optimal trade-off among performance, feasibility, and integration constraints. This consolidated design includes the following key features:

– Rear Zone: replacement of ACB and beryllide with OLP
– Cooling Plates: increased thickness to 8 mm
– First Wall: addition of a 1 cm ACB layer
– Structural Reinforcement: inclusion of a 2 cm toroidal Eurofer steel stiffener

This configuration is detailed in Section 7, along with the corresponding TBR and nuclear heating results, which provide essential input for the next phase of thermal–hydraulic analyses.

2. Input data

For the neutronic modelling and analyses, the recommendations described in the *Neutronic guidelines* [6] have been followed. They specify the computational tools and data to be applied, the neutron source, materials specifications, calculation techniques to be used and targeted accuracies to be achieved. Some of the most important ones are summarized here:

(1) DEMO parameters

The overall operation parameters of the DEMO reactor are taken from the PROCESS run of May 3rd, 2017 [7] which corresponds to the so-called DEMO 2017. The main parameters are given in Table 2.1.

(2) Requirements

The requirements followed for tritium breeding are those defined in [8] which establish a target for the Tritium Breeding Ratio (TBR) $\geq$ 1.15.

(3) Codes and data

The analyses included in this task have entailed the use the Monte Carlo code MCNP5v1.6 [9] and the nuclear cross sections from JEFF3.2 nuclear data libraries [10] for the transport simulations. All results obtained from the Monte Carlo simulations have relative uncertainties less than 0.03 %. The proposed modifications of the BB have been prepared through MCNP and visualized by MCAM (Monte Carlo Modeling Interface Program) tool SuperMC_3.3.1 Professional Version [11].

Table 2.1
Main DEMO1 parameters.

Parameter	Unit	Value
Plasma power	MW	1998
n source particles per seconds	n/s	7.094e20
Thermal power including n-multiplication in blanket	MW	2634
Plant electricity output capability	MW	500
Lifetime neutron damage in steel in the FW	dpa	20 + 50[i]
Major radius	m	8.938
Minor radius	m	2.883
Number of toroidal field coils		16
Plasma current	MA	19.075
Toroidal field at R_0	T	4.890
Elongation, κ_{95}		1.65
Triangularity, δ_{95}		0.33
Plasma volume	m^3	2466
Average neutron wall load	MW/m^2	1.036
Nuclear heating in blanket	MW	1565
Power to divertor	MW	183.8

[i] Limits concerning the 'starter' DEMO phase to withstand 1.57 FPY and the 'second' DEMO phase to withstand 4.43 FPY for a total of 6 FPY.

3. WLCB BB cassettes reference model

The starting neutronic model used as reference for the further modifications has been developed on the basis of the sketch shown in Fig. 3.1. The BB unit is then integrated (Fig. 3.2) inside the generic DEMO model with "universes" and "fills" structures for easily plugging of the different BB unit versions developed herein and studied.

The WLCB BB consists of a multilayer FW composed of a 2 mm plasma-facing surface of tungsten, a 2.5 cm Eurofer wall, embedded with cooling channels. In the neutronic MCNP model, this is simplified as a 0.3 cm Eurofer layer + 0.7 cm water layer + 1.5 cm Eurofer layer. The FW casing is reinforced to safely ensure the blanket integrity against a Loss of Coolant Accident (LOCA): the plasma faced FW part is 2.5 cm thick and the sidewalls are 7 cm thick.

A 21 cm Back Supporting Structure (BSS), inside which the cooling water manifolds are located, includes 3 cm back wall of the BZ and three feeding water channels separated by the steel walls.

The BZ is 75 cm thick at the Outboard (OB) equatorial plane and 53.6 cm at the Inboard (IB) equatorial zone. The BZ is formed by repeating vertical cassettes, which structure has been varied according to the studies described in Sections 4-7.

The toroidal thickness of each chamber originally 11 cm, has been broken down as 8.5 cm Pb, 2 cm ACB and 0.5 cm CPs in the starting configuration.

The Advanced Ceramic Breeder (ACB) is made by Li_4SiO_4 + 35 % mol. Li_2TiO_3 in pebbles form (64 % vol. fraction) and is placed in vertical cassettes orthogonal to the FW as it is shown in Fig. 3.2 (in blue colour). The ^{6}Li enrichment is set to 90 % as it is adopted in all breeder blanket designs based on the PbLi liquid metal technology. The space of the adjacent cassettes to the ACB ones is filled with molten Pb (in pink colour in Fig. 3.2). The cooling plates (in yellow in Fig. 3.2) have water cooling channels.

A shape and dimensions of these channels are not yet fixed and they will be defined in subsequent studies. As a preliminary option, a 50 %/50 % steel/water mixture was used in the model. All structural elements in the WLCB blanket are made of Eurofer steel.

4. Design challenges and parametric campaign 2022–23

The initial WLCB BB cassette configuration (v1), described above, yielded a Tritium Breeding Ratio (TBR) of 1.098—significantly below the target value of 1.15 [8].

To address this shortfall, a dedicated parametric campaign was launched in 2022–23 with the objective of optimizing the WLCB BB design from a neutronic perspective. The primary focus was on enhancing Tritium breeding performance, which remains the core function of the breeding blanket and a fundamental requirement for the feasibility of a self-sustaining fusion power plant.

A summary of the parametric studies carried out to increase the TBR – that will be fully described in next sections –. concerned the:

– Sizing and layout of the ACB and Pb layers: check best thickness combination (Section 4.1)
– Modification of the Back zone replacing part of the Pb by ACB, with different sizes (Section 4.2)
– Modification of the Back zone replacing Pb by reflectors of C (graphite) or $Be_{12}Ti$, with different sizes (Section 4.3)
– Modification of the Back zone including a full layer of reflectors of C or $Be_{12}Ti$ of different size (Section 4.4)
– Radial resizing of the back zone with different material combinations option (Section 4.5)

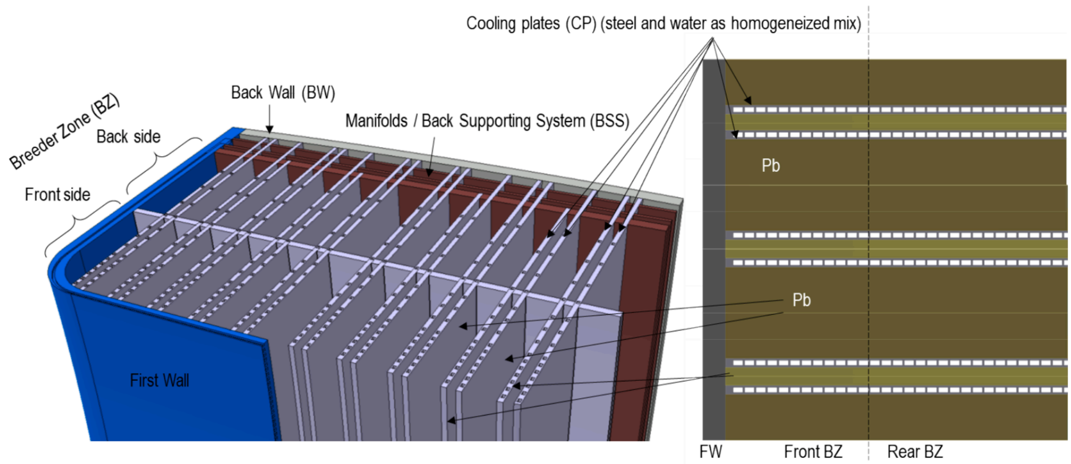

Fig. 3.1. Sketch of the WLCB BB cassettes configuration.

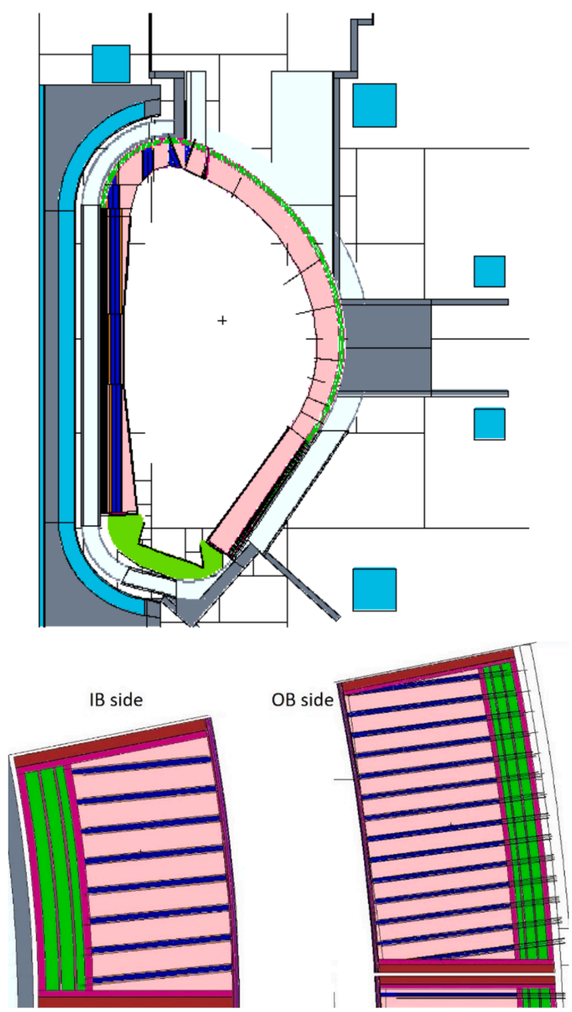

Fig. 3.2. Visualization by MCNP plot interface of the WLCB BB cassettes configuration neutronic model integrated inside the generic DEMO model: (up) vertical cut; (down) horizontal cut at IB and OB equatorial zone.

4.1. Parametric study for the sizing and layout of the Pb/ACB layers

To address the limited Tritium breeding performance of the initial WLCB configuration, a dedicated parametric campaign was carried out with the aim of identifying an optimal layering strategy in terms of the size and number of alternating Pb and ACB layers. As part of this effort, 11 additional configurations were developed. A subset of these is partially illustrated in Fig. 4.1, which shows schematic representations of the repeated unit structures for four selected configurations. The corresponding TBR values are reported in Table 4.1. The figure includes the reference configuration (v1), followed by a series of variants (v2 to v8) in which the ACB layer thickness is progressively increased from 2 cm to 5.5 cm (2, 2.5, 3, 3.5, 4, 4.5, 5, and 5.5 cm), while the Pb thickness is correspondingly reduced from 8.5 cm to 5 cm (8.5, 8, 7.5, 7, 6.5, 6, 5.5, and 5 cm). For all these configurations, the cooling plate (CP) thickness was maintained at 0.5 cm.

In Table 4.1 the specific thickness of the Pb and ACB layers is given per each configuration v1-v8 together with the TBR results and its relative variation in comparison with the baseline v1. Such TBR results are also displayed in Fig. 4.2. where it is easily identifiable the maximum value that is achieved with configurations v3 and v4. Version v3 has 7.5 cm and 3 cm thickness of the Pb and ACB layers and version v4 has 7 cm and 3.5 cm for Pb and ACB layers, respectively. Version v3 is highlighted in orange inside the table, since it produces the highest TBR (1.1148) and will be used as reference for further modifications and parametric studies as described in next sections. Such TBR result supposes an increase of a 1.49 % from the starting configuration (1.098).

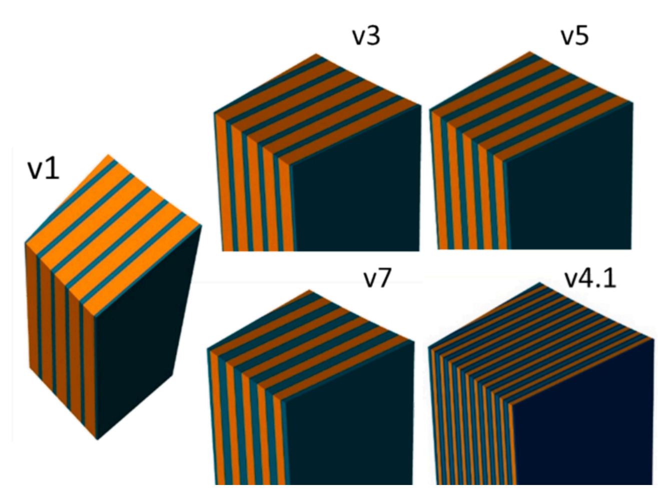

Fig. 4.1. WLCB BB unit layout of Pb and ACB layers in the starting configuration v1, and progressively increasing the ACB thickness. In v4.1 the layers of ACB and Pb are doubled. In version v5.1 (not displayed) Pb and ACB layers are inverted respect to v4.1. Blue: cooling plates; Orange: Pb; Green: ACB. (For interpretation of the references to colour in this figure legend, the reader is referred to the web version of this article.)

Table 4.1
TBR variation according to different layering configurations of Pb and ACB with 0.5 cm CP.

	Pb/ACB thickness (cm)	TBR	% over v1
v1	8.5/2	1.0984	------
v2	8/2.5	1.1102	1.07%
v3	7.5/3	**1.1148**	1.49%
v4	7/3.5	1.1147	1.49%
v5	6.5/4	1.1105	1.11%
v6	6/4.5	1.1035	0.47%
v7	5.5/5	1.0940	-0.40%
v8	5/5.5	1.0824	-1.46%
	0.5 cm cooling plate		

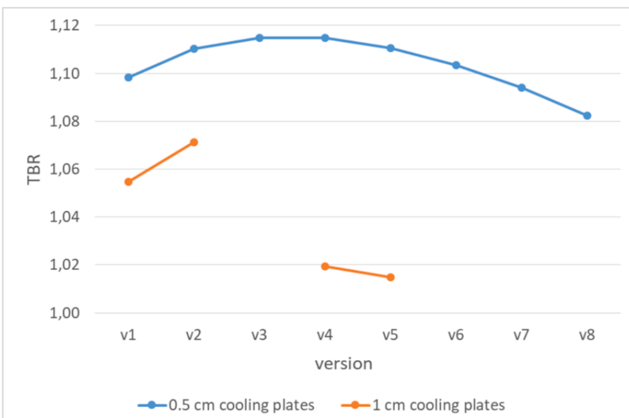

Fig. 4.2. TBR results for versions v1-v8 with 0.5 cm cooling plates (blue curve) and versions v1.1, v2.1, v4.1 and v5.1 with 1 cm cooling plates (orange curve). (For interpretation of the references to colour in this figure legend, the reader is referred to the web version of this article.)

Table 4.2
TBR variation according to different layering configurations of Pb and ACB with 1 cm CP.

	Pb/ACB thickness (cm)	TBR	% over v1
v1.1	7.5/2	1.0549	-3.96%
v2.1	8/1.5	1.0713	-2.47%
v4.1	Double layers: ACB 1.75cm, Pb 2cm	1.0193	-7.20%
v5.1	Double layers: ACB 2cm, Pb 1.75cm	1.0149	-7.60%
1 cm cooling plate			

An additional set has been also tested increasing the thickness of the cooling plates to 1 cm. Just four configurations have been assessed due to the strong negative impact of such increase on the TBR (Table 4.2). In v1.1 it has been kept the ACB original thickness to 2 cm but the increase of the cooling plates thickness has been practiced at the expense of the Pb thickness reduced from 8.5 to 7.5 cm. Such version has the strongest impact on the TBR implying a reduction of nearly a 4 % from v1.

In v2.1 it has been kept the Pb thickness of version v2 (8 cm) but the increase of the cooling plates thickness has been practiced at the expense of the ACB thickness of v2 reduced from 2.5 to 1.5 cm. The reduction of the TBR has been a 2.5 % demonstrating in certain measure the importance of the Pb as neutron multiplier.

In v4.1 (Fig. 4.1), the layers of ACB and Pb have been doubled, so that in the same space there are 10 Pb layers instead than 5 but with reduced thickness (ACB 1.75 cm, Pb 2 cm). In v5.1 (not displayed) Pb and ACB layers are inverted respect to v4.1 (ACB 2 cm, Pb 1.75 cm). Both versions imply a reduction of more than a 7 % over the baseline TBR. This is due to the increase of steel layers in the doubled configurations.

In Fig. 4.2. the TBR results produced by using both series of models have been plotted, providing a very clear picture of the negative impact of using 1 cm cooling plates.

Due to all these considerations, v3, which produced the best TBR result, was furtherly used for the subsequent neutronic optimizations.

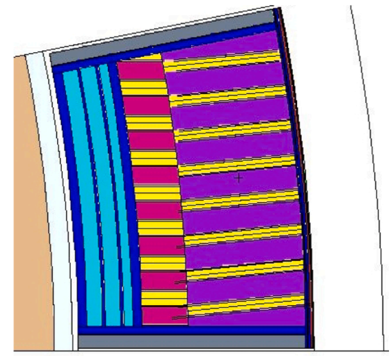

Yellow: ACB, 15_35 cm IB_OB v3_v6

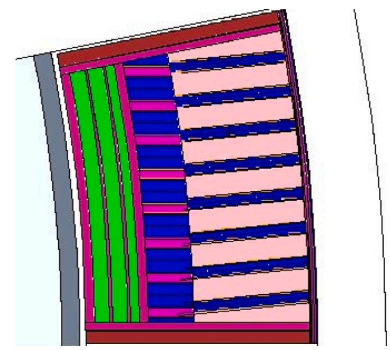

Blue: ACB, 15_35 cm IB_OB v3_v9

Fig. 4.3. Visualization by MCNP plot interface of the WLCB BB versions v3_v6 and v3_v9 at the eq. IB plane.

4.2. Back zone modification replacing part of Pb by ACB

As a continuation of the cassette configuration optimization, an additional study was conducted focusing exclusively on modifications to the back zone of both the Inboard (IB) and Outboard (OB) Breeding Zones (BZ). In this analysis, the front zone configuration was held constant, corresponding to the parameters of version v3.

The back zone, however, was varied by implementing configurations previously developed in versions v6 and v8, along with a newly defined version, v9. Specifically, a 15 cm radial segment was modified in the IB region, and a 35 cm radial segment was altered in the OB region, applying these distinct layered structures.

As a result, three new cassette configurations were developed and evaluated.

- Configuration v3_v6 with:
  7.5 cm Pb and 3 cm ACB in the front

Table 4.3
TBR variation employing v3 in the front and varying the layering configurations of ACB and multiplier/reflector in the rear zone.

15cmIB_35cmOB	total	% over prev.	% over v3
v3_v6_Pb	1.1197	0.44%	0.44%
v3_v8_Pb	1.1227	0.27%	0.71%
v3_v9_Pb	1.1254	0.24%	0.95%
v3_v6_$Be_{12}Ti$	1.1290	0.83%	1.27%
v3_v8_$Be_{12}Ti$	1.1305	0.70%	1.41%
v3_v9_$Be_{12}Ti$	**1.1310**	0.50%	1.46%
v3_v6_C	1.1231	-0.52%	0.74%
v3_v8_C	1.1247	-0.52%	0.89%
v3_v9_C	1.1283	-0.24%	1.21%

6 cm Pb and 4.5 cm ACB in 15 cm of the IB back zone and in 35 cm of the OB back zone

- Configuration v3_v8:
  7.5 cm Pb and 3 cm ACB in the front
  5 cm Pb and 5.5 cm ACB in 15 cm of the IB back zone and in 35 cm of the OB back zone

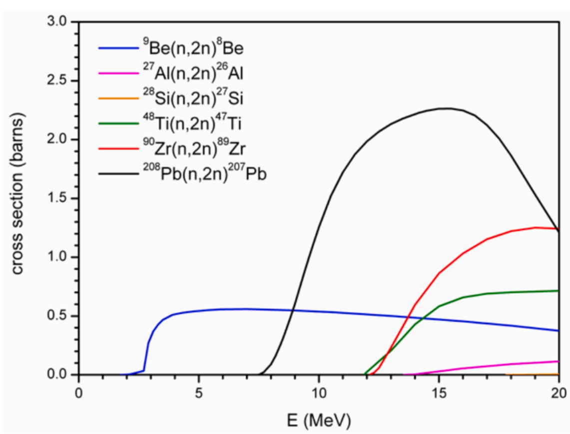

Fig. 4.4. Comparison of (n,2n) reactions for different n multiplier isotopes by using ENDF/B-VII cross section data library, as taken from [12].

Table 4.4
TBR variation employing v3 in the front and a full layer of multiplier/reflector in the rear zone.

v3 (front)	$Be_{12}Ti$ full reflector layer (back)	
	TBR	% over v3
3 cm	1.1154	0.06%
15 cm	1.1007	-1.26%
v3 (front)	C full reflector layer (back)	
	TBR	% over v3
3 cm	1.1145	-0.03%
15 cm	1.1055	-0.83%

- Configuration v3_v9:
  7.5 cm Pb and 3 cm ACB in the front
  3 cm Pb and 7.5 cm ACB in 15 cm of the IB back zone and in 35 cm of the OB back zone

In this last case it was deemed both feasible and beneficial to increase the thickness of the ACB layer up to 7.5 cm in the back breeding zone. This approach had not been considered for the front breeding zone in previous campaigns due to two main constraints: 1) thermal considerations – a thicker ceramic in the front could lead to excessively high temperatures, potentially compromising material integrity; 2) neutronic performance – in the front region, where neutrons are still energetic, the presence of Pb is essential for its neutron multiplying capability. In contrast, in the back region, Pb contributes far less to neutron multiplication due to the slowed neutron spectrum. Additionally, the ACB in the rear zone is not expected to reach critical temperatures, as it resides deeper in the blanket structure where thermal loads are reduced.

The new configurations, shown in Fig. 4.3 as MCNP plots at the equatorial IB plane region, reflect these adjustments. The corresponding TBR results, along with the percentage variation relative to version v3, are presented in Table 4.3 (highlighted in orange). The highest TBR was achieved with configuration v3_v9, yielding an increase of nearly 1 % over v3, and reaching an absolute TBR value of 1.125.

4.3. Pb replaced by C or $Be_{12}Ti$ in the back zone

In this study the Pb multiplier has been substituted with a reflector material such as graphite (C) or a titanium beryllide ($Be_{12}Ti$) just in the back zone of 15_35 cm IB_OB.

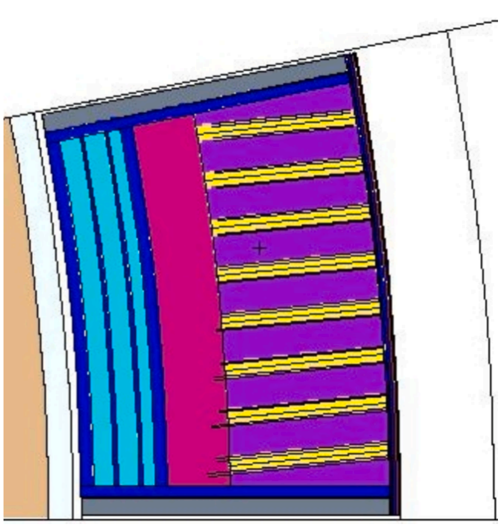

Fig. 4.5. Visualization by MCNP plot interface for the version v3 with a 15 cm full reflector layer.

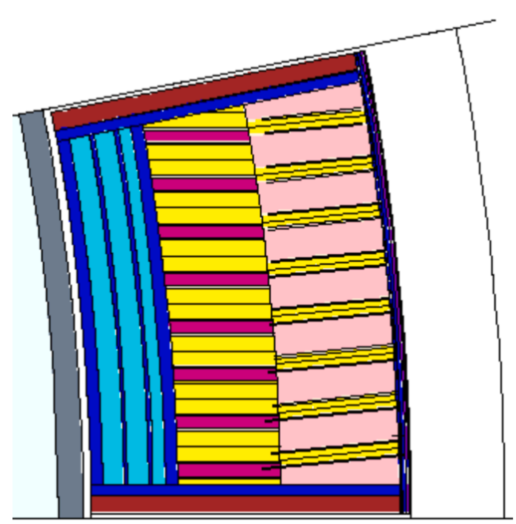

Fig. 4.6. Visualization of the v3_v9 version with 25_45 cm radial layouts for the IB_OB (*baseline2022*).

Table 4.5
TBR variation with the radial thickness of the front/rear zone while considering Pb (orange) for v3_v6 or $Be_{12}Ti$ (purple) for v3_v9.

IB_OB cm	total	% over v3_v6
15_40	1.1200	0.03%
15_45	1.1202	0.05%
20_40	1.1203	0.05%
25_45	**1.1207**	0.09%
IB_OB cm	total	% over v3_v9_Be12Ti
25_45	**1.1325**	0.13%

The results for the six new configurations are given in Table 4.3 (purple and blue rows). TBR absolute values are provided together with the relative variations. From the table, it is possible to observe that the best material working as good reflector and also good neutron multiplier in the back zone is $Be_{12}Ti$, providing a TBR of 1.131 in the v3_v9 case. This material works better than Pb in such zone, since the Be threshold for $^{9}Be(n,2n)^{8}Be$ reactions is around 1.86 MeV instead than the 7 MeV of $^{208}Pb(n,2n)^{207}Pb$ reactions (Fig. 4.4).

4.4. Full layer of C or $Be_{12}Ti$ introduced in the back zone

The possibility of using graphite (C) or titanium beryllide ($Be_{12}Ti$) as a continuous, full-layer reflector in the back zone of the breeding blanket—rather than as interlayers between the ACB layers—was investigated. Two layer thicknesses were considered to fill the breeding zone: 3 cm and 15 cm. The MCNP plot of the configuration with a 15 cm full-layer reflector is shown in Fig. 4.5. The corresponding results, summarized in Table 4.4 (deep purple and deep blue values), indicate that this substitution does not improve the TBR in any scenario.

While the 3 cm $Be_{12}Ti$ reflector shows a slight TBR increase compared to v3, the overall conclusion is that placing the reflector as an interlayer between ACB layers is more effective than using a full continuous layer. This is because the reduction in ACB volume from the full-layer reflector configuration outweighs the TBR gains provided by the reflector material.

4.5. Radial resizing of the back zone

The last set of configurations consisted in modifying the radial thickness of the back zone from the starting 15 cm IB and 35 cm OB sides regions. For the case of v3_v6 with Pb as multiplier, 4 different radial

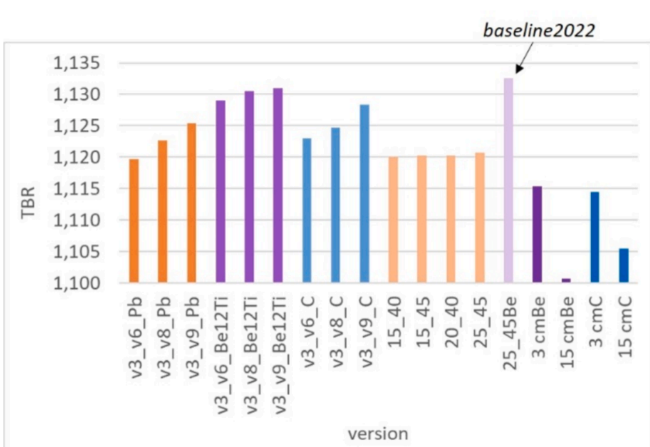

Fig. 4.7. TBR variation for 18 configurations of the first Campaign. The maximum value corresponds to the established *baseline2022* used for further optimizations.

sizes have been testes being:

- 15 cm and 40 cm,
- 15 cm and 45 cm,
- 20 cm and 40 cm and
- 25 cm and 45 cm

for the IB and OB sides, respectively.

For the case of v3_v9 with $Be_{12}Ti$ multiplier in the back zone, which previously provided the best results among all the tested configurations, just the maximum size of 25_45 cm IB_OB back zones has been tested (Fig. 4.6.), to get the maximum value achievable with such campaign.

The results are summarized in Table 4.5 (light orange and light purple values). From the data it is possible to observe that the radial thickness change of the back region implies a moderate increase in the TBR results if we compare with the previous cases with 15_35 cm IB_OB. In fact, the TBR increase in any of the configurations with v3_v6 is less than 0.1 % and with v3_v9 in the best of the cases (with 25_45 radial thickness increase) is 0.13 % respect to the size 15_35. The maximum TBR value achieved in this first neutronic campaign was 1.1325, representing an increase of over 3 % from the initial value of 1.0984.

The campaign's outcomes justified selecting this improved version as *baseline2022*, which has since served as the foundation for subsequent development and enhancements in later campaigns.

A summary picture of the TBR values of 18 configurations of the 30 developed in this campaign is shown in Fig. 4.7.

4.6. Tritium production and nuclear heating 3D analyses

A full comparison between the initial and last configurations of such campaign has been carried out, providing the full maps of the T produced in the two cases, as 3D mesh tally plots, shown in Fig. 4.8.

From that it is possible to observe that the efficiency of T breeding in the back zone has been increased significantly by increasing the ACB volume and using beryllide as neutron multiplier.

Furthermore, for the last version v3_v9_$Be_{12}Ti$ in order to give inputs to the subsequent thermal–hydraulic analyses the nuclear heating profiles inside the different materials of the WLCB unit have been computed. The radial profiles shown in Fig. 4.9a represents the nuclear heating results inside the cooling plates front zone (line 8), rear zone (line 10), the Pb in the front and the $Be_{12}Ti$ in the rear zone (line 12) and in the ACB (line 18). Such profiles have been taken from the global mesh tally displayed in Fig. 4.9b. The mesh tally has been produced with a very high resolution, employing bins of 0.5 cm × 0.2 cm × 10 cm in XYZ directions, respectively, for a total number of 1.200.000 voxels, in order to be able to differentiate among very thin layers (CP, n multipliers, ACB).

5. Parametric campaign 2023–24

Several studies and modifications have been afforded under this campaign to furtherly optimize the T breeding performance but also to answer special design requirements, for example: thermal–hydraulic constraints, cost reductions associated with ^{6}Li enrichment process, and minimizing reliance on beryllium. A sketch of the zones affected by modifications, described in next sections, is given in Fig. 5.1. The ideas proposed have been the following:

i. Modify the cooling plates
ii. Add a neutron multiplier block at the front side
iii. Modify the rear ceramic zone

In particular, the modifications and studies carried out concerned the analyses with:

(1) different Cooling Plates water content

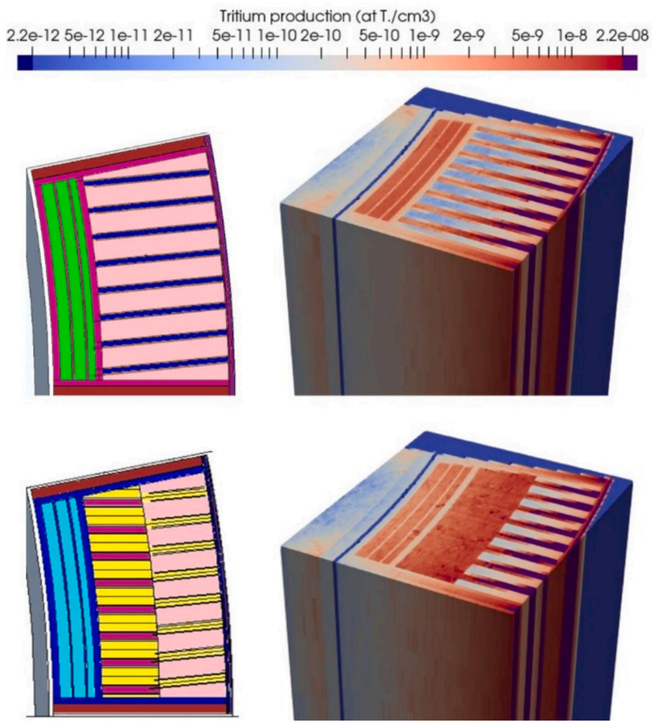

Fig. 4.8. 3D maps mesh tally of the T production efficiency (as at. T/cm^3) in the IB side for the starting (up) and last (down) cassettes configurations adopting a very high resolution.

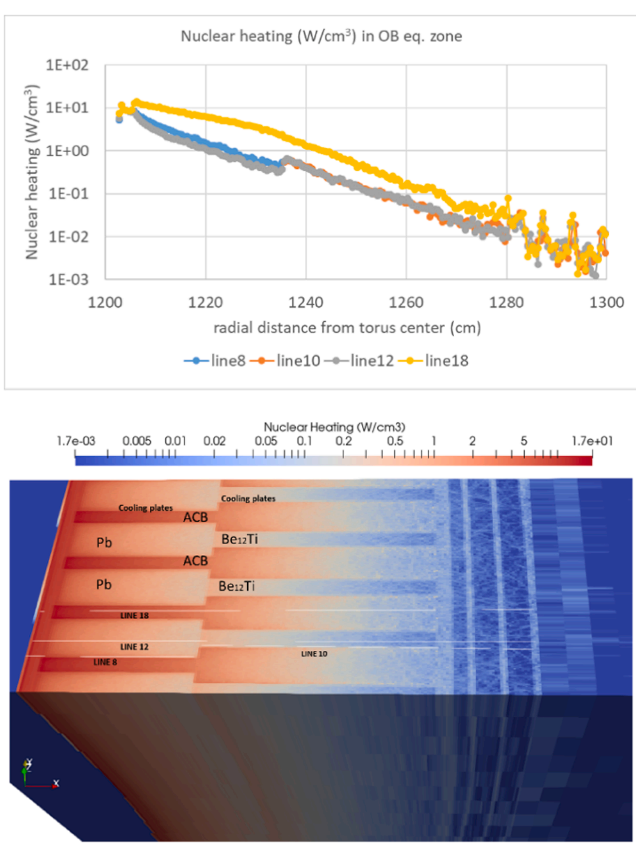

Fig. 4.9. a) Nuclear heating profiles in the different materials of the wlcb bb cassettes baseline; (b) entire mesh tally 3d map in the whole ob equatorial zone from which the profiles of (a) have been taken.

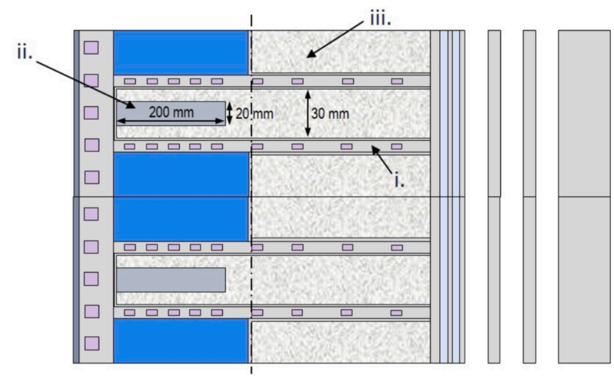

Fig. 5.1. Zones affected by modifications during campaign 2023–34.

(2) different ^{6}Li enrichments
(3) different CP thicknesses in front/rear BB zones
(4) introduction of a multiplier block at the front side replacing the ACB – by testing two different materials ($Be_{12}Ti$, Zr_5Pb_3), different block sizes and CP thickness.
(5) replacing part of the $Be_{12}Ti$ at the rear by ACB and testing different packing factors
(6) different ACB packing factors in front/rear zones
(7) substitution of ACB in the rear with Li_8PbO_6 (OLP) testing different packing factors
(8) substitution of beryllide at the rear zone with OLP
(9) substitution of front ACB with OLP

5.1. Cooling plate water content

Different WLCB configurations have been created by modifying the % of water and Pb in the cooling plates (from the initial v.0 that uses 50 % Eurofer/50 % water):

(0.1) 50 % Eurofer + 25 % water + 25 % Pb;
(0.2) 50 % Eurofer + 18 % water + 32 % Pb;
(0.3) 50 % Eurofer + 10 % water + 40 % Pb.

The objective was to assess the effect of reducing the water content without re-designing the geometry of each cooling plate, which would otherwise require adjusting its thickness to prevent overheating. Instead, this effect was simulated "virtually" by replacing part of the water with Pb, maintaining the same geometry. Such virtual modifications of material composition are a common neutronics practice to approximate geometric changes efficiently.

These compositions have been tested for two configurations explored in the previous 2022–23 campaign: Configuration v3_v9 with:

- 7.5 cm Pb and 3 cm ACB in the front
- 3 cm **Pb** and 7.5 cm ACB in **15** cm of the IB back zone and in **35** cm of the OB back zone
- 0.5 cm cooling plates, (named here as **V1.0**)

and Configuration v3_v9 similar to the previous but with 3 cm $\mathbf{Be_{12}Ti}$ and 7.5 cm ACB in **25** cm of the IB back zone and in **45** cm of the OB back zone, being the *baseline2022* version (**V2.0** in Table 5.1) considered as reference for most of the studies.

The results are shown in Table 5.1 (first row results) and in Fig. 5.2. The CP option (0.1) with 50 % Eurofer + 25 % water + 25 % Pb composition shows a slight increase in the TBR, especially interesting for V2 here furtherly explored, respect to the achieved with the (0.0) CP composition with 50 % water. Composition (0.2) provide similar values than (0.1), while increasing more the Pb content at the expense of the

Table 5.1
Summary table with the TBR results for 8 parametric studies and 61 configurations tested during the Campaign 2023–24 (test 5.3 not displayed).

Section	^{6}Li (%)	v1.0	v2.0	v1.1	v2.1	v1.2	v2.2	v1.3	v2.3
5.1.	90	1.1254	**1.1325**	1.1281	**1.1370**	1.1263	**1.1370**	1.1237	1.1367
5.2.	85	1.1220	1.1298	1.1224	1.1319	1.1203	1.1316	1.1171	1.1311
	80	1,1163	1,1246	1,1161	1,1265	1,1138	1,1259	1,1097	1,1250
	75	1,1102	1,1191	1,1095	1,1204	1,1064	1,1194	1,1019	1,1182

Section 5.4.

Be$_{12}$Ti block	TBR	Zr$_5$Pb$_3$ block	TBR
20x2 cm^2 front - 1cm CP	1.0889	20x2 cm^2 front	
1 cm CP front, 0.5 cm CP rear	1.0934	1 cm CP front, 0.5 cm CP rear	1.0619
0.5 cm front, 0.5 cm rear	**1.1354**	0.5 cm CP front 0.5 cm CP rear	1.0973
full block 30x2 cm^2 1 cm CP front, 0.5 cm CP rear	1.0834		

Section 5.5

at. density ACB	7.44E-02	8.14E-02	8.72E-02	9.30E-02	9.88E-02	1.05E-01
Packing Factor ACB	PF 64%	PF 70%	PF 75%	PF 80%	PF 85%	PF 90%
front zone PF modified	0.851	0.867	0.879	0.890	0.900	0.909
back zone PF modified	0.194	0.185	0.178	0.172	0.165	0.159
replaced beryllide with ACB	0.078	0.074	0.071	0.068	0.065	0.063
Total TBR	1.123	1.126	1.128	1.129	1.130	1.131

Section 5.8	at. density	TBR
ACB front 64%PF	7.44E-02	0.843
OLP rear 90%PF	1.04E-01	0.212
OLP rear 90%PF replacing beryllide	1.04E-01	8.31E-02
Total TBR		**1.1374**

Section 5.6.

Packing Factor ACB	PF 64% *baseline2022*	PF 70%	PF 75%	PF 80%	PF 85%	PF 90%
fixed front zone at 64% PF	0.8677	0.8674	0.8670	0.8666	0.8662	0.8658
rear zone PF **modified**	0.2648	0.2663	0.2671	0.2679	0.2687	0.2693
Total TBR	**1.1325**	**1.1336**	**1.1341**	**1.1345**	**1.1349**	**1.1352**

front zone PF **modified**	0.8679	0.8826	0.8938	0.9037	0.9131	0.9216
rear zone PF modified	0.2648	0.2517	0.2416	0.2320	0.2232	0.2147
Total TBR	**1.1327**	**1.1343**	**1.1355**	**1.1358**	**1.1363**	**1.1363**

Section 5.9.	Li$_8$PbO$_6$ PF 90%	
	at density	TBR
front OLP	1.04E-01	0.975
rear OLP	1.04E-01	0.213
Total TBR		**1.1881**

Section 5.7.	Li$_8$PbO$_6$ PF 64%		PF 70%		PF 75%		PF 80%		PF 85%		PF 90%	
	at density	TBR	at density	TBR	at density	TBR	at density	TBR	at density	TBR	at density	TBR
front ACB	7.44E-02	0.861	7.44E-02	0.860	7.44E-02	0.859	7.44E-02	0.859	7.44E-02	0.859	7.44E-02	0.858
rear OLP	7.39E-02	0.279	8.09E-02	0.280	8.66E-02	0.281	9.24E-02	0.282	9.82E-02	0.283	1.04E-01	0.284
Total TBR		**1.1392**		**1.1400**		**1.1406**		**1.1411**		**1.1415**		**1.1419**

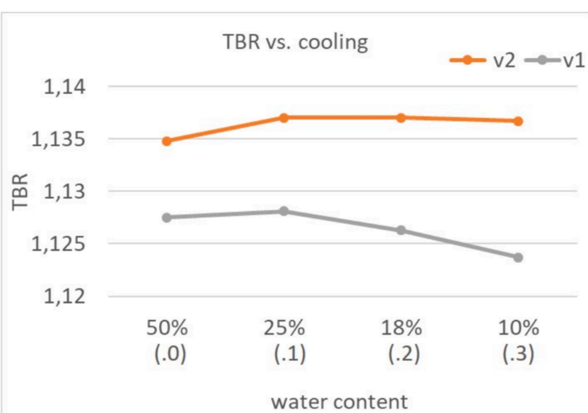

Fig. 5.2. TBR results of V1 and V2 configurations employing different CP mixture from 10 to 50% water.

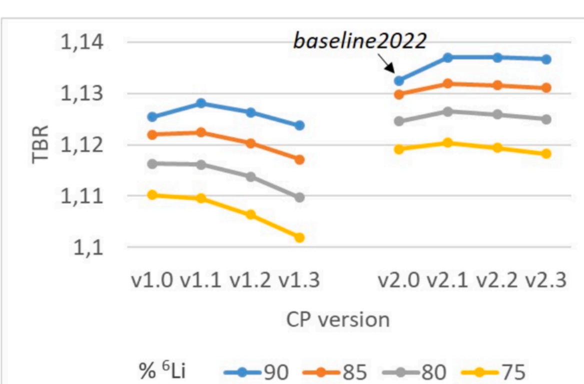

Fig. 5.3. TBR results of 32 configurations of the second campaign employing V1 and V2, different CP mixture from 10 to 50% water and Li-6 enrichments from 75 to 90%.

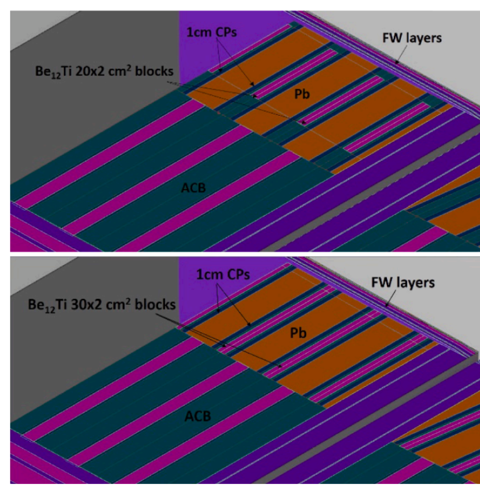

Fig. 5.4. Introduction of an additional n multiplier block (pink) inside the ACB front zone (green duck): a) partial coverage block of 20x2 cm^2; b) a full coverage block of 30x2cm^2. (For interpretation of the references to colour in this figure legend, the reader is referred to the web version of this article.)

water (0.3) produces a TBR decrease so that a sort of maximum is found around the composition (0.1).

5.2. Li-6 enrichment

Different ^{6}Li enrichment have been tested (75—80 – 85—90 %) with the objective to verify if a lower ^{6}Li enrichment could be suitable to avoid costly enrichment processes. The two configurations V1.0 and V2.0 described above have been explored again together with the 4 CP options explored in point 5.1.

The results are shown in Table 5.1 (rest of rows) and Fig. 5.3. The table shows that a 10 % reduction in ^{6}Li content inside the ACB reduces around 1 % the TBR, resulting still unfeasible for the configurations here analyzed. Such TBR reduction slightly increase at higher Pb content

(0.3).

5.3. Cooling plate thickness

A series of tests were conducted by progressively increasing the CP thickness to address thermal–hydraulic needs:

(a) from 0.5 cm to 1 cm at the front, and
(b) from 0.5 cm to 1 cm across the entire radial depth.

The results using these CPs over version V2.0 *baseline2022* have been 1.0877 and 1.0927 in the two cases a and b, respectively, indicating a reduction of −3.95 % in the first case (a) and an additional −0.45 % more in case (b).

These findings underscore the significant influence of CP thickness on the TBR, highlighting the challenges in optimizing the cooling system design. A dedicated thermal–hydraulic study is currently underway to explore the potential for minimizing CP thickness and reducing steel fraction as much as possible.

5.4. Neutron multiplier block

With the objective of improving the tritium breeding performance of such WLCB configurations another component has been introduced in the front zone. For that, 6 additional configurations have been prepared combining the use of a neutron multiplier block with the CP configurations adopted in study 5.3. The primarily chosen neutron multiplier has been $Be_{12}Ti$. For that two different sizes have been selected: a small block (20 cm x 2 cm as in Fig. 5.4a) occupying partially the front zone, or a larger block (30 cm x 2 cm) occupying completely (Fig. 5.4b) the front zone. Also, different CP thickness have been tested for the front and rear zones. In the first case the best TBR result is achieved by considering again a CP of 0.5 cm in the full radial depth (1.1354). Such value means a 0.26 % more than the *baseline2022* (1.1325). The use of a full block of $Be_{12}Ti$ proves less favorable compared to a partial coverage block, for which just one CP configuration has been tested in such case. The TBR results for all the combinations are given in Table 5.1.

Another neutron multiplier material, Zr_5Pb_3, with density of 8.8 gr/cm^3 as reported in [13], has been also tested. However, due to its negative impact on the TBR (Table 5.1), only two tests were ultimately conducted. The limited effectiveness of Zr_5Pb_3, compared to the superior results obtained with $Be_{12}Ti$, can be explained by examining the (n,2n) reaction threshold shown in Fig. 4.4. Here a comparison of (n,2n) reactions for different neutron multiplier isotopes is provided as taken from [12]. The threshold energy for the ^{9}Be(n,2n)^{8}Be reactions is approximately 1.86 MeV, which is significantly lower than the 12.3 MeV threshold for the ^{90}Zr(n,2n)^{89}Zr reactions (being this one similar to that of the Ti used in the beryllide). Such energy threshold for Zr could be too high given the energy spectrum of incident neutrons (max 14 MeV which degrade as they penetrate further into the BB).

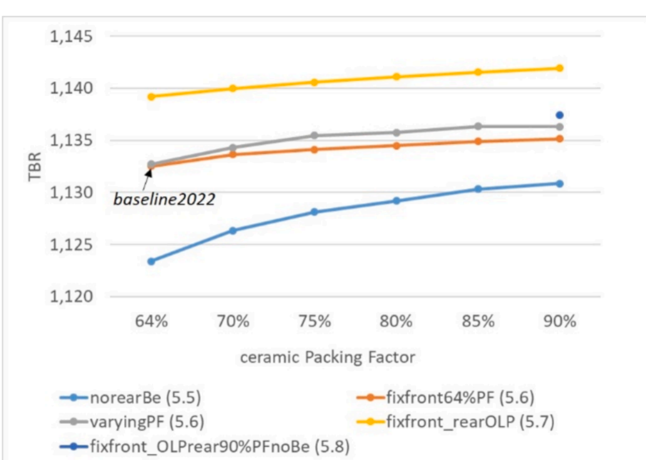

Fig. 5.5. TBR variation for 24 configurations of the second Campaign at different PF compared to the *baseline2022*.

Table 5.2
Lithium density of different ceramic breeders.

material	Theor.density (g·cm^{-3})	Li at.density (cm^{-3})
Li_8PbO_6	4.24	5.7×10^{22}
Li_4SiO_4	2.40	4.8×10^{22}
Li_2TiO_3	3.43	3.8×10^{22}
Li_2SiO_3	2.53	3.4×10^{22}
Li_2ZrO_3	4.15	3.3×10^{22}
$LiAlO_2$	2.65	2.4×10^{22}

5.5. Back zone modification replacing $Be_{12}Ti$ by ACB and employing different ACB packing factors

In this study, the beryllide neutron multiplier in the rear zone was replaced with the ACB. Various packing factors (PF) were evaluated for the ACB, ranging from the initial 64 % up to 90 %—a value considered feasible according to [14]. The results for each of the six new configurations are presented in Table 5.1 and Fig. 5.5 (blue curve). Although increasing the PF leads to an improvement in the TBR, the overall values remain significantly lower than the *baseline2022* TBR of 1.1325. This reduction is primarily due to the decreased volume of the neutron multiplier. Given the critical role of a large multiplier fraction in the back zone of the breeding blanket, this approach is not recommended for further exploration.

5.6. Modification of ACB packing factor

The same exercise has been repeated here but without the n multiplier suppression. Instead, the study focused on testing:

(a) different ACB PF just in the rear zone, or
(b) in both rear and front zone,

starting from the PF of 64 % of the baseline up to 90 % [14].

The results for the new 11 configurations together with the baseline are given in Table 5.1 and Fig. 5.5 (orange and grey curves). TBR total values are provided together with the breakdown front/rear zone. From the table, it is possible to observe that at higher PF, higher TBR, as it could be expected, and the use of increasing PF in the whole radial depth produce increasing the TBR up to 1.1363, a 0.34 % more than the baseline. Moreover, passing from 90 % PF rear to both rear and front zone implies an increase of 0.1 %.

5.7. Back zone modification using OLP instead than ACB at different PF

The option of using another ceramic breeder instead of the ACB has been explored here by employing Li_8PbO_6 (Octa-Lithium-Plumbate, OLP). This compound has been previously considered in breeding blanket design studies for DEMO [15,16], owing to several advantageous properties:

- it possesses the highest stoichiometric lithium content among candidate ceramics (Table 5.2)[12]
- the presence of lead provides inherent neutron multiplication, potentially reducing or even eliminating the need for additional moderation and the inclusion of beryllium as a neutron multiplier.
- tritium exhibits high diffusivity in irradiated OLP samples [17,18], leading to low residence times within the ceramic, which is favorable for both safety and fuel self-sufficiency.

Hence, due to the high Li atomic density and the neutron-multiplying capability of lead, OLP appears to be superior to the ACB (Li_4SiO_4 + Li_2TiO_3). However, despite its promise in terms of tritium breeding, octalithium compounds are known to be thermally unstable at elevated temperatures [19,20]. Many decompose below 1000 °C, and Li_8PbO_6 may exhibit similar behavior. For this reason, OLP has been preliminarily tested only in the rear zone of the blanket, where operating temperatures are lower.

Different PFs for such ceramic have been also tested from 64 % to 90 %. According to the results of Table 5.1 for the 6 configurations developed the increase in the TBR is considerable (Fig. 5.5 yellow curve) since it reaches a value of 1.1419, in the best of the cases, which is near to the 1.15 TBR target and a 0.82 % higher tan the initial 1.1325. In fact, if we sum up to such increase (0.82 %), the increase due to the use of higher PF ACB in the front (0.1 %), the increase by using a n multiplier block (0.26 %) and CP (0.1) composition (0.2 %) the global increase from the starting 1.1325 could be around 1.38 %, that would allow achieving a TBR of 1.148 very near to the TBR target of 1.15.

5.8. Substitution of beryllide at the rear zone with OLP

This modification involved altering the beryllide in the rear zone using OLP, following a similar approach to that described in Section 5.5. However, in this case, OLP was applied (and just at 90 % PF) – instead of ACB – which include the Pb neutron multiplier.

Once again, the outcome is somewhat counterproductive (Table 5.1 and blue dot in Fig. 5.5), as the TBR drops to 1.1374 — lower than a comparable configuration without this beryllide substitution and with a reduced OLP PF of 64 %, which yielded a TBR of 1.1392. Nevertheless, this result still exceeds the *baseline2022* value, making it noteworthy from the perspective of reducing reliance on beryllium as a neutron multiplier.

A full summary picture of the TBR results achieved from the 25 configurations described in Sections 5.5–5.8 is given in Fig. 5.5.

5.9. Substitution of front ACB with OLP

As an extreme case a last test was conducted assuming a 90 % PF on

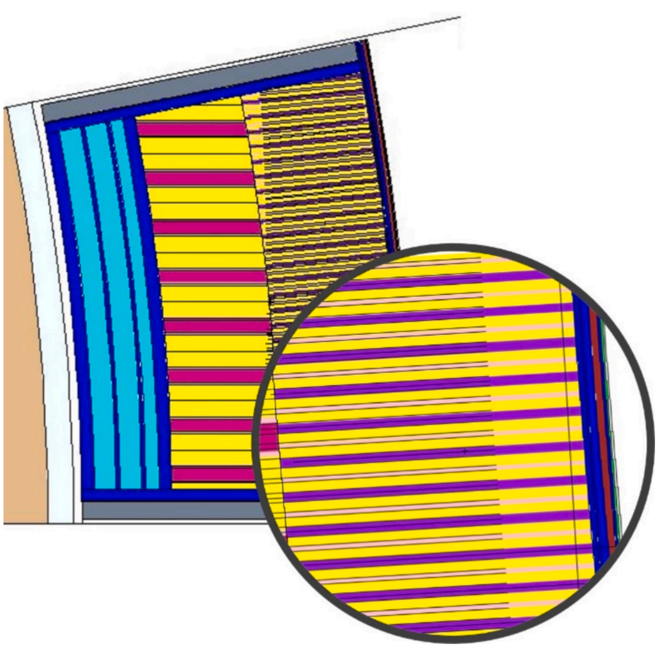

Fig. 6.1. WLCB BB MCNP model with 1 cm Pb layers (purple) in the repeated novel structure in the front BZ. (For interpretation of the references to colour in this figure legend, the reader is referred to the web version of this article.)

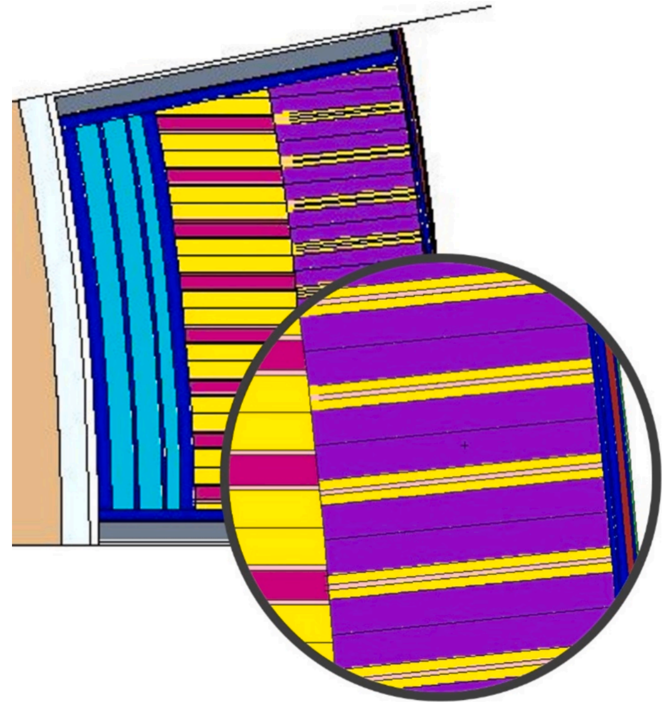

Fig. 6.2. WLCB BB novel MCNP model with 7 cm Pb front layer (purple colour), 2 cm ACB (yellow) and 0.5 cm CP (light pink) inside the ACB filling the resultant 9.5 cm new repeated unit structure. (For interpretation of the references to colour in this figure legend, the reader is referred to the web version of this article.)

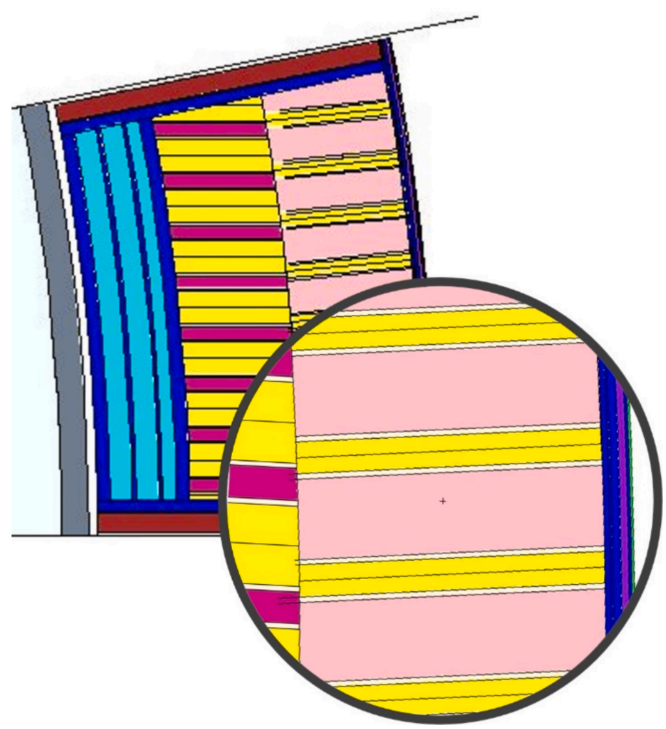

Fig. 6.3. WLCB BB *baseline2022* MCNP model with 7.5 cm Pb front layer (salmon colour), 3 cm ACB (yellow) and two 0.5 cm CPs (light yellow) at the two ACB sides filling the previous 11 cm repeated unit structure. (For interpretation of the references to colour in this figure legend, the reader is referred to the web version of this article.)

Table 6.1
Summary table with the TBR results for 8 parametric studies and 58 configurations tested during the Campaign 2024–25 compared with *baseline2022* (7 mm CP test not displayed).

Multiplier thickness	***baseline 2022***	Pb_New_ BeTi_Old (0.1)*	Pb_BeTi New unit (0.2)	Pb_ACB New unit (0.3)	Pb_Pb New unit (0.4)	Pb_C New unit (0.4)	Pb_ZrH_2 New unit (0.4)	OLP (0.5)**	8 mm CP (0.6)	1 cm ACB FW (0.7)	Toroidal Plate (0.8)
1 cm		1.0478	1.0502	1.0356	1.0429	1.0350	1.0434				
2 cm		1.1033	1.1109	1.0921	1.0989	1.0897	1.0969				
3 cm		1.1315	1.1411	1.1207	1.1242	1.1169	1.1172				
4 cm		1.1457	1.1548	1.1356	1.1332	1.1289	**1.1183**				
5 cm		1.1532	**1.1650** *baseline 2024*	1.1434	**1.1360**	1.1358	1.1104	**1.188**	1.1504	**1.179**	**1.1505**
6 cm		1.1547	1.1611	1.1450	1.1307	1.1363	1.0982				
7 cm		**1.1568**	1.1612	**1.1473**	1.1280	**1.1380**	1.0859				
7.5 cm	1.1325										
8 cm		1.1509	1.1476	1.1418	1.1132	1.1285	1.0591				
9 cm		1.1499	1.1272	1.1410	1.0991	1.1169	1.0251				

* newUnitFrontPb, oldUnitBeTiBack.
** Front_ACB + OLP + Pb; Back_OLP + $Be_{12}Ti$.

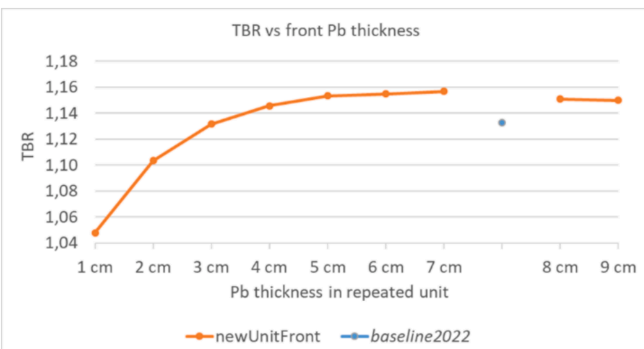

Fig. 6.4. TBR vs Pb layer thickness in the new layout applied to the front zone (orange curve) and in the *baseline2022* 7.5 cm Pb unit (blue point). (For interpretation of the references to colour in this figure legend, the reader is referred to the web version of this article.)

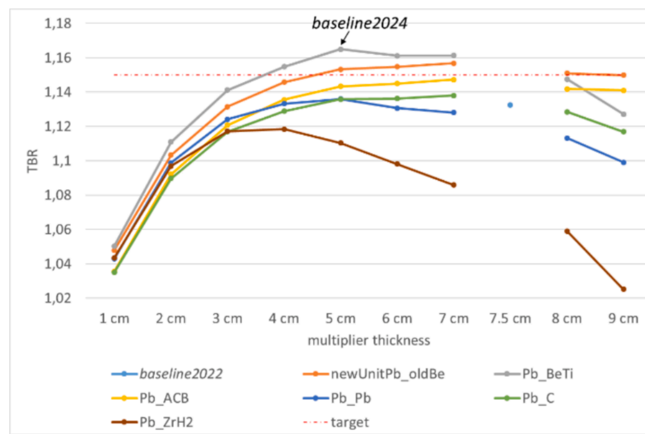

Fig. 6.5. TBR variation with the multiplier thickness for 54 configurations of the third Campaign compared with the *baseline2022* with 7.5 cm Pb unit (blue dot): new layout applied to front zone (orange curve), front and rear (grey), using just ACB in the rear without n multiplier (yellow), or employing Pb (blue), C (green) or ZrH_2 (brown) n multiplier. The maximum value corresponds to the established *baseline2024* used for further optimizations. (For interpretation of the references to colour in this figure legend, the reader is referred to the web version of this article.)

OLP material applied in both the front and rear zone. This modification resulted in a substantial increase of the TBR to 1.188 (+4.29 %) as shown in Table 5.1. However, the feasibility of using OLP in the front region remains to be confirmed due to potential thermal stability concerns.

6. Parametric campaign 2024–25

During this campaign, both novel solutions and previously implemented in campaigns 2022–23 and 2024–25 have been tested, now applied with slight variations. The campaign began with modifications to the front unit layout, as detailed in the following section.

6.1. Modification of the front unit layout (parametric study with fixed 1 cm ACB and variable 1 cm to 9 cm Pb)

In this key test, the basic 11 cm "unit" structure repeated within the breeding zone (BZ) was redesigned using an alternative configuration. Instead of placing the 0.5 cm cooling plate (CP) on either side of the ACB, it was relocated to the center of the ceramic layer. This central positioning reduces the use of steel in the breeder zone that would have a positive impact on the T production. The ceramic layer itself was fixed at 2 cm in total thickness, with the 0.5 cm CP embedded in the middle, ensuring a consistent configuration across all cases. A parametric study was then conducted by varying the thickness of the Pb layer from 1 cm to 9 cm. This variation determines the number of unit structures needed to toroidally fill the BZ, with thinner Pb layers allowing for more repetitions and thicker ones resulting in fewer.

The MCNP neutronic models with 1 and 7 cm Pb are displayed in Fig. 6.1. and 6.2, respectively. The difference between the *baseline2022* model with 7.5 cm Pb and the most comparable configuration using the new layout (with 7 cm Pb) can be deduced observing Figs. 6.2 and 6.3 (new layout and old, respectively).

The TBR results for the new 9 cases are given in Table 6.1 and depicted in Fig. 6.4 together with the *baseline2022* result of 1.1325 (blue dot). With more than 3 cm Pb the new layout is working better than the *baseline2022* and the maximum TBR (1.1568) is reached with 7 cm Pb, providing an increase of more than 2 %. The TBR target of 1.15 is reached since version with 5 cm Pb.

The new layout and the best model achieved with 7 cm Pb, 2 cm ACB and 0,5 cm CP inside the ACB layer has been furtherly adopted for testing additional modifications, namely:

(2) Application of new unit layout to the rear zone
(3) Use of ACB in the rear zone without n multiplier
(4) Use of Pb, C and ZrH_2 in the rear zone instead of beryllide
(5) Use of 100 % OLP in the rear zone and mixture of 50 % ACB + 50 % OLP in the front
(6) Cooling plates modification from 5 mm to 7–8 mm

(7) FW modifications with additional 1 cm layer ACB
(8) Toroidal stiffener 2 cm steel

described in the following sections.

6.2. Application of new unit layout to the rear zone

The new layout has been adopted also in the rear zone, providing a general slight improvement of the responses (Fig. 6.5 grey curve), but comparatively not so pronounced as the improvement given by the new layout applied to the front zone. The peak value is slightly moved: from 7 cm Pb to the version using 5 cm Pb which provides a TBR of **1.165** (Table 6.1). This model will be furtherly used for additional modifications for which it has been named as *baseline2024*.

6.3. Use of ACB in the rear zone without n multiplier

In this test applied to the previous systematic study (6.2) with novel front and rear layouts, the ACB has been employed to fill completely the rear zone substituting the beryllide neutron multiplier $Be_{12}Ti$ with the ceramic breeder similarly to what described in Section 5.5. In such case, as previously occurred, the TBR is in general slight reduced (yellow curve of Fig. 6.5 and results of Table 6.1) but still quite feasible producing a peak of 1.1473 around the configuration with 7 cm front Pb.

6.4. Use of Pb, C and ZrH_2 in the rear zone

In this study, alternative neutron multipliers were evaluated as potential substitutes for beryllide. The materials considered were lead (Pb, blue curve in Fig. 6.5), graphite (C, green curve), and zirconium hydride (ZrH_2, brown curve). However, all three options yielded inferior results compared to beryllide—and even compared to the ACB configuration without any neutron multiplier (see Table 6.1). As a result, these alternatives were discarded.

A complete summary picture of the TBR results achieved for the 54 configurations described in Sections 6.1–6.4 of the third Campaign is given in Fig. 6.5.

Summarizing the maximum TBR values in increasing order are: 1,118 with 4 cm ZrH_2; 1,136 with 5 cm Pb; 1,138 with 7 cm C; 1,1473 with 7 cm ACB; 1,165 with 5 cm $Be_{12}Ti$ (1.1654 considering also Tritium produced in Be) – *baseline2024*.

Generally, the T produced in the $Be_{12}Ti$ has been not added in the TBR calculation for the sake of conservativism, due to the uncertainties of the release of this tritium from $Be_{12}Ti$. Nonetheless in the case of the

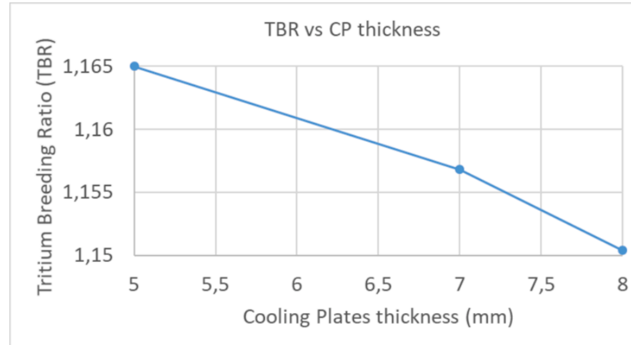

Fig. 6.7. TBR vs CP thickness in the new *baseline2024*.

baseline2024 it has been computed simply to demonstrate that using Be in such small amount just in the rear zone would not play a role in achieving the TBR target making unnecessary its recovery for the T fuel cycle standpoint.

6.5. Use of 100 % OLP in the rear zone and mixture of 50 % ACB + 50 % OLP in the front

Given the positive results obtained in earlier tests, the Advanced Ceramic Breeder (ACB) has been also replaced with Octa-Lithium Plumbate (OLP) in the new layout configuration. In particular, in this context, a mixture of ACB + OLP (at 50 % each one) has been employed in the front zone and a full OLP BZ has been applied in the rear zone, due to possible temperature issues of the OLP in the front. For both, a packing factor of 64 % has been conservatively chosen. This case has been tested just with the layout with 5 cm Pb layers in the front and 5 cm $Be_{12}Ti$ layers in the rear zone (*baseline2024*). The resulting TBR has been 1.188 (Table 6.1) more than a 2 % higher than the value of 1.1650 achieved with the same layout but standard ACB ceramic in both front and back zone (*baseline2024*).

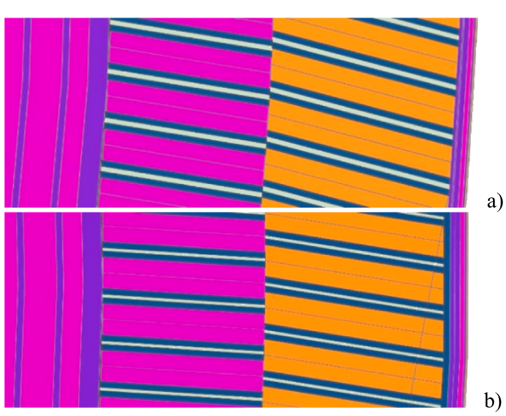

Fig. 6.6. Zoomed IB equatorial section of the WLCB model visualized in SuperMC: (a) the *baseline2024* model modified with a thicker CP (grey) layer in the middle of the ACB layer (deep-blue) and (b) the *baseline2024* model modified with an additional ACB layer (deep blue) behind the FW layers (orange + pink + purple). (For interpretation of the references to colour in this figure legend, the reader is referred to the web version of this article.)

Fig. 6.8. IB equatorial section of the *baseline2024* configuration with an additional stiffening steel layer (clear blue) between the front and rear BZ visualized in SuperMC. (For interpretation of the references to colour in this figure legend, the reader is referred to the web version of this article.)

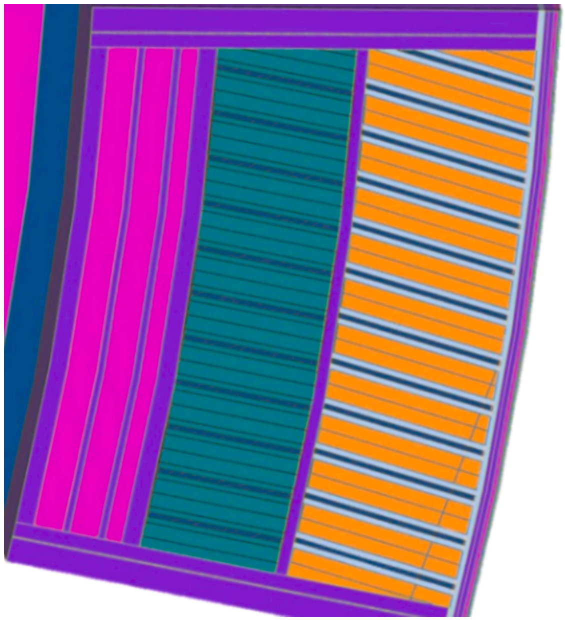

Fig. 7.1. Final configuration based on *baseline2024* (5 cm Pb new layout) with an additional stiffening steel layer (purple) between the front and rear BZ, CP of 0.8 mm (blue), full OLP material (green-duck) in the rear zone (with no external n multiplier) and additional 1 cm ACB (light blue) behind the FW. (For interpretation of the references to colour in this figure legend, the reader is referred to the web version of this article.)

6.6. Cooling plates modification from 5 mm to 7–8 mm

In this test, an important modification has been implemented to the *baseline2024* model with the new unit in front and back, and 5 cm multiplier that employs cooling plates (CP) of 5 mm thickness. This component has demonstrated to play a critical role in meeting the TBR target since 1 cm thickness suggested by preliminary thermal–hydraulic studies would imply a detrimental impact on such a crucial parameter. As a compromise, an intermediate and more realistic solution employing 7 or 8 mm CP thickness has been proposed, while maintaining a water content of 50 % in the cooling system.

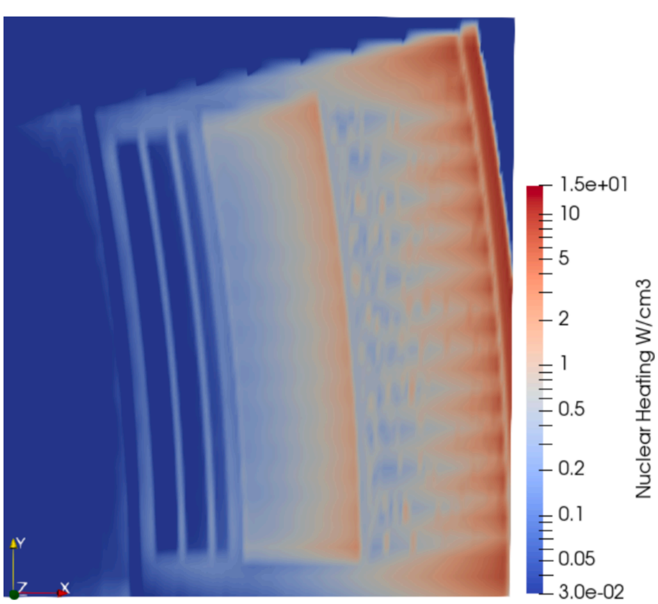

Fig. 7.2. Nuclear Heating 3D map (as W/cm^3) at the IB equatorial section of the WLCB model visualized in ParaView for the final case.

A SuperMC sketch of the modified model with thicker CP is depicted in Fig. 6.6a. where a thicker grey component, the CP, is visible inside the ACB layer (in deep blue colour).

In this case, the TBR passes from 1.165 with 5 mm CP to 1.1568 with 7 mm CP and to 1.1504 with 8 mm CP (almost a variation of 0.5 % each mm). A clear picture of the variation of the TBR with the CP thickness for the *baseline2024* model is provided in Fig. 6.7 where such strong dependency is shown. Nonetheless the 1.15 target would be still achieved with 8 mm CP.

6.7. Addition of 1 cm front layer of ACB

An innovative modification has been proposed in this case working on the First Wall (FW) design. In such study, behind the standard FW layers an additional layer of 1 cm ACB has been included. The modification is shown in Fig. 6.6b where a specific zoom showing the difference between the standard FW *baseline2024* model (a) and such new variation is given. The achieved TBR (Table 6.1) is 1.179, more than a 1 % higher than the *baseline2024* value (1.165) and a 2 % higher than the 1.15 target, generating some extra margin for the application of other modifications that could negatively impact the result.

6.8. Toroidal stiffener of 2 cm steel

The last modification introduced was among the most controversial, as it was expected to negatively affect the TBR but necessary for mechanical integrity. A 2 cm toroidal stiffening plate made of Eurofer steel was incorporated into the neutronic model, using the *baseline2024* configuration. The model is shown in Fig. 6.8. in which a clear-blue layer is observed in the IB section separating the front BZ: ACB (blue) + Pb (orange); and the rear BZ: ACB (blue) + $Be_{12}Ti$ (pink). The TBR in this case, passes from 1.165 to 1.1505, being slightly over the target.

7. Final case. TBR and nuclear heating studies

A final case has been developed based on the most promising but also the required modifications tested separately in previous sessions. The model (Fig. 7.1.) integrate together the:

- New unit with 5 cm multiplier
- Use of OLP in the rear zone instead of ACB + $Be_{12}Ti$
- Cooling plates of 8 mm
- FW modification with additional 1 cm layer ACB
- Toroidal stiffener of 2 cm steel

In this case, the TBR decreases slightly from 1.165 to approximately 1.160 (1.1596), maintaining a margin of about 1 % above the 1.15 target and thus representing a viable solution from a neutronic standpoint.

However, this design requires further evaluation from a thermal–hydraulic perspective as a priority. To this end, nuclear heating has been calculated in the IB equatorial region to determine the power deposited in the various blanket materials. In Fig. 7.2. it is possible to observe the 3D maps created from the mesh tally results of the total nuclear heating due to neutron + photon components in a slice of the BB located in the IB equatorial plane at z = 0.

Additionally, radial profiles are depicted in Fig. 7.3 as responses given per material, each 2 cm in toroidal direction (Y) to catch the different elements/materials. Different scales are provided (logarithmic (a) /linear (b)) as well as different radial ranges, being depicted in (a) the full radial profile from 580 cm to 440 cm from the plasma, which implies from the FW to the BSS or in (b) a partial profile from 580 to 520 cm identifying just the BZ region for a better visualization of the results.

The yellow and grey curves belong to Pb layers, orange belong to ABC, blue to the cooling plate. In any case following the X direction the resulting profiles are not perfectly aligned with the orientation of the BB layers, which may lead to minor interferences between materials. As

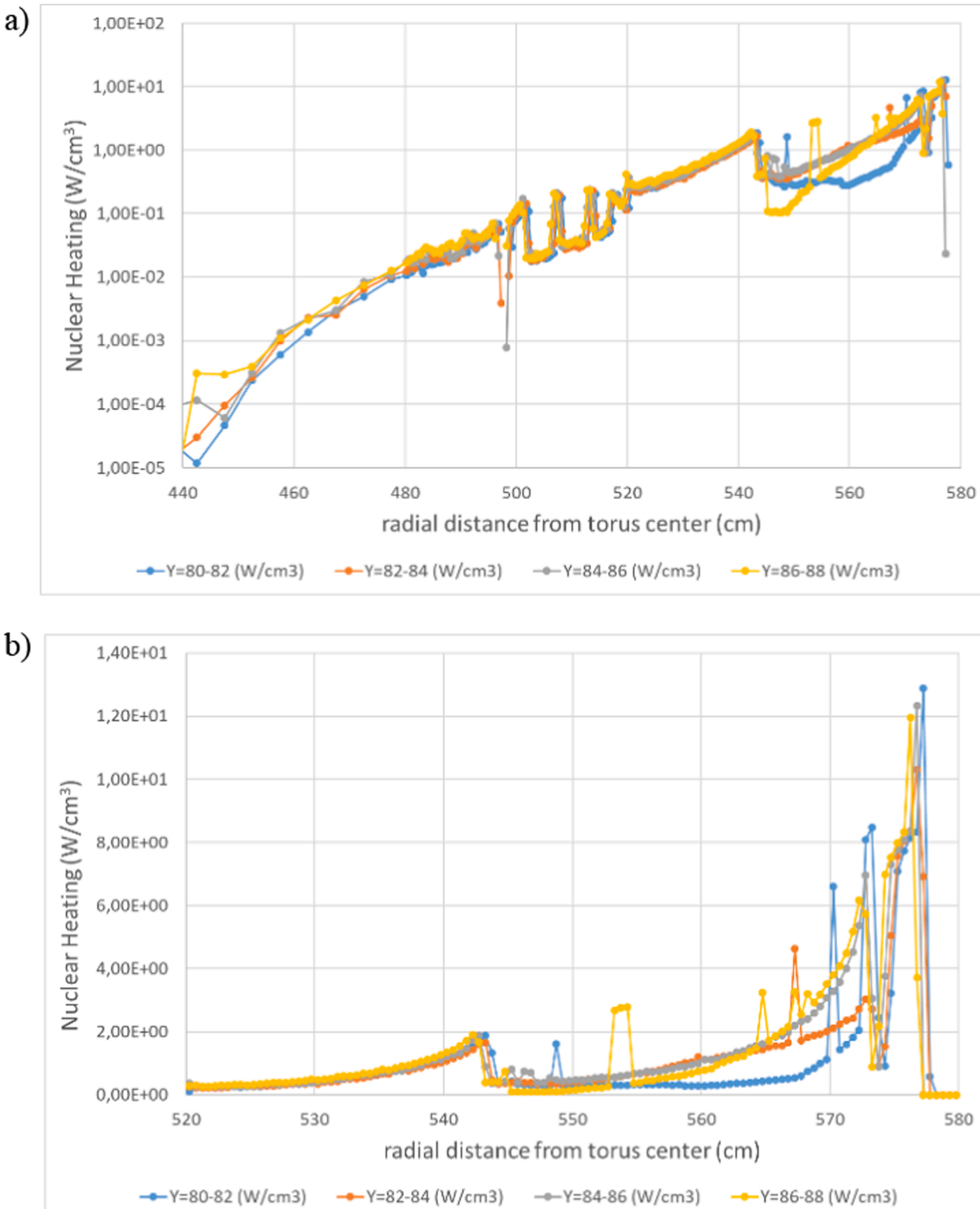

Fig. 7.3. Radial profiles of the Nuclear Heating as W/cm^3 in the different components of the BB. The yellow and grey curves belong to Pb layers, orange belong to ABC, blue to the cooling plate; a) logarithmic scale; b) linear scale in reduced radial range just to cover the BZ. (For interpretation of the references to colour in this figure legend, the reader is referred to the web version of this article.)

illustrated in figure (b) noticeable differences between the curves appear in the front zone (575–545 cm approx.) that gradually disappear in the rear zone.

8. Discussion and Conclusions

As support to the study of alternative configurations of Breeding Blanket (BB) for the European DEMO fusion reactor, aimed at overcoming the open issues that emerged at the end of the Pre-Conceptual Design (PCD) phase, for the HCPB and WCLL *driver blankets*, a new concept, called *Water-cooled Lead and Ceramic Breeder* (WLCB), has been proposed and here examined and optimized under the T breeding perspective.

A vertical cassettes configuration alternating advanced ceramic breeder (ACB) and the neutron multiplier (Pb, in first instance) separated by vertical cooling plates (steel cooled by water) has been optimized under neutronic point of view, performing a comprehensive neutronic campaign in order to find configurations to maximize the TBR and attain a promising design solution.

Hence, a number of parametric studies have been carried out modifying: the size and number of repeated vertical structures, radial separation of the front and rear regions, modification of neutron multiplier (Pb, $Be_{12}Ti$, C, ZrH_2), of ceramic breeder (ACB and OLP), of the cooling plates thickness and water cooling fraction, and FW modification among other studies.

During the first campaign (30 configurations tested) a strong improvement was observed when passing from v1 (with 8.5/2 cm of Pb/ACB layers) to v3 (with 7.5/3 cm of Pb/ACB layers) than used as reference for further improvements. Then adopting a v9 configuration in the back (3 cm Pb and 7.5 cm ACB in 15 cm and 25 cm radial zone for the IB and OB sides, respectively) with $Be_{12}Ti$ multiplier instead then Pb provided further increase up to 1.131. This has been furtherly improved up to 1.1325 (*baseline2022*) by enlarging the back zone to 25 cm IB and 45 cm OB. Such value supposes an increase of more than 3 % from the original value of 1.0984.

During the second campaign, which included a total of 63 configurations, the most significant improvement was achieved by replacing the ACB with OLP in the rear zone and employing a higher packing fraction (PF). This change increased the TBR from the *baseline2022* value of 1.1325 to 1.1419 (+0.82 %). When combined with other tested enhancements — such as a higher PF ACB in the front zone (+0.1 %), the addition of a neutron multiplier block (+0.26 %), and using CP with improved composition (+0.2 %) — the overall TBR increase could reach approximately 1.38 %. This would potentially raise the TBR to about 1.148, very close to the target of 1.15.

In the third campaign, comprising 59 configurations, a new unit layout was tested in which the cooling plate was positioned in the middle of the ACB rather than having two at its sides. This modification generally increased the TBR across several tested variants, reaching 1.165 (*baseline2024*) with 5 cm of Pb. This configuration was subsequently refined by exploring different multipliers, ceramic materials, first wall designs, and other factors.

As general observations:

- alternative neutron multipliers to beryllide did not yield improvements
- OLP consistently enhanced TBR compared to ACB and also compared to ACB + berillyde
- thicker cooling plates and the introduction of a toroidal stiffening wall negatively impacted TBR but were considered affordable when applied to optimized designs to reflect minimum size requirement of a cooling plate channel (minimum length $\approx$5mm), as well minimum thickness due to structural reasons (mainly due to segment pressurization in an in-box LOCA).

A final case has been created merging the different options to find the best tradeoff between all the solutions, resulting in a design with:

- OLP in the rear zone instead of ACB and beryllide,
- Cooling plates of 8 mm,
- FW with additional 1 cm layer ACB,
- Toroidal stiffener of 2 cm steel.

In this case, the TBR decreases slightly from 1.165 to 1.1596 ($\sim$1.16), maintaining a margin of approximately 1 % above the target value of 1.15 and achieving total independence from beryllium as a neutron multiplier. This confirms the viability of this solution from a neutronic perspective. For this configuration, nuclear heating calculations were also performed to provide input for subsequent analyses and further optimization of the model will follow through iterative integration with thermal–hydraulic and mechanical assessments.

Overall, the results indicate that the WLCB breeding blanket cassette configuration does not present any showstopper from tritium breeding requirement standpoint. There remains sufficient margin to accommodate additional modifications that may arise from ongoing mechanical and thermal–hydraulic studies.

The model is going to be adapted to the updated DEMO LAR (Low Aspect Ratio) design and it has recently been selected within the European Fusion Roadmap as the leading near-term breeding blanket concept for further in-depth development under the WPBB programme.

CRediT authorship contribution statement

Iole Palermo: Writing – review & editing, Writing – original draft, Visualization, Software, Methodology, Investigation, Formal analysis, Data curation, Conceptualization. **Francisco A. Hernandez:** Writing – review & editing, Supervision, Resources, Project administration, Funding acquisition, Conceptualization. **Salvatore D'Amico:** Supervision, Conceptualization. **Jin Hun Park:** Software, Resources. **Pavel Pereslavtsev:** Software, Resources. **Guangming Zhou:** Writing – review & editing, Validation, Conceptualization. **Iñaki Zumalde:** Software, Formal analysis, Data curation.

Declaration of competing interest

The authors declare that they have no known competing financial interests or personal relationships that could have appeared to influence the work reported in this paper.

Acknowledgments

This work has been carried out within the framework of the EUROfusion Consortium, funded by the European Union via the Euratom Research and Training Programme (Grant Agreement No 101052200 — EUROfusion). Views and opinions expressed are however those of the author(s) only and do not necessarily reflect those of the European Union or the European Commission. Neither the European Union nor the European Commission can be held responsible for them. The work has been also partially developed in the framework of the E4XTREM project, ref. PLEC2024-011136, funded by MICIU/ AEI/ 10.13039/ 501100011033/ FEDER, UE.

Data availability

Data will be made available on request.

References

[1] G. Federici, et al., An overview of the EU breeding blanket design strategy as an integral part of the DEMO design effort, Fusion Eng. Des. 141 (2019) 30–42.
[2] F. Hernández, et al., Advancements in Designing the DEMO driver Blanket System at the EU DEMO Pre-Conceptual Design phase: Overview, Challenges and Opportunities. Journal Nucl. Eng. 4 (3) (2023) 565–601.
[3] G. Zhou, et al., A Water cooled Lead Ceramic Breeder blanket for European DEMO, Fusion Eng. Des. 168 (2021) 112397.
[4] I. Palermo, DES-ENG.NUCENG.NUCAN-T003-D002 Technical Report for ANALYST.NUC.3 / Nuclear (Neutronic) Analyst 2022 on WLCB tubes configurations EFDA_D_2PWQ6G.
[5] P. Pereslavtsev, EFDA_D_2NVU8L-Technical Report on Neutronic analyses of the WCLL "double bundle".
[6] U. Fischer, Guidelines for neutronic analyses, EFDA_D_2L8TR9 v1.8, 2020.
[7] DEMO1 PROCESS output (May 2017), EFDA_2NDSKT_v1_0.
[8] U. Fischer, et al., Required, achievable and target TBR for the European DEMO. Fusion Eng. Des. 155 (2020) 111553.
[9] X-5 Monte Carlo Team, MCNP – A general Monte Carlo N-Particle Transport Code, Version 5.
[10] The JEFF-3.2 Nuclear Data Library, NUCLEAR ENERGY AGENCY, OECD.
[11] Y. Wu, FDS Team, CAD-based interface programs for fusion neutron transport simulation, Fusion Eng. Des. 84 (2009) 1987–1992.
[12] I. Palermo, et al., Preliminary neutronic assessment of a helium-cooled Li_8PbO_6 breeding blanket design for DEMO, 26th Symposium on, Fusion Technol. (2010).

[13] M. Dalle Donne, et al., Fabrication and properties of Zr_5Pb_3, a new neutron multiplier material for fusion blankets, Journal Nucl. Mat. 141–143 (1986) 369–372.

[14] S. Sharafat, et al., Development of a new cellular solid breeder for enhanced tritium production, Fusion Eng. Des. 109–111 (2016) 119–127.

[15] I. Palermo, et al., Preliminary neutronic assessment of a helium-cooled Li_8PbO_6 breeding blanket design for DEMO, Fus. Eng. and Des. 87 (2012) 195–199.

[16] S. Colominas, et al., Octalithium plumbate as breeding blanket ceramic: Neutronic performances, synthesis and partial characterization, Fus. Eng. and Des. 87 (5–6) (2012) 482–485.

[17] S. Konishi, et al., Investigation of lithium diffusion in octalithium plumbate by conductivity and NMR measurements, J. Am. Ceram. Soc. 73 (1990) 1710–1713.

[18] T. Hayashi, S. Konishi, K. Okuno, Tritium release behaviour from neutron irradiated Li8PbO6, J. Nucl. Mater. 170 (1990) 60–65.

[19] B. Brazel, et al., Zur Kristallstruktur von Li8PbO6, Zeitschrift für anorganische allgemeine, Chemie 514 (1984) 81–86.

[20] F.A. Hernández, P. Pereslavtsev, First principles review of options for tritium breeder and neutron multiplier materials for breeding blankets in fusion reactors, Fus. Eng. and Des 137 (2018) 243–256.